Wang HU, Zhang QIAOGEN, Wei JIN, Liu XUANDONG, Qiu AICI

School of Electrical Engineering, Xi'an Jiaotong University, 710049, Xi'an, Shaanxi Province, China.

Research on Thermal Conduction Mechanism on Electrode Surface in Field-distortion Gas Switch Discharging

Abstract. *Pulsed power technology is one of the technological foundations in high and new technology research, which has extremely broad development and application prospect. Gas switch is one of the key elements in pulsed-power devices, and electrode erosion is a key restrictive factor in high-power gas switch development and application. According to one dimensional equation of heat conduction and thermal equilibrium equation near the electrode surface, this paper researches electrode heat conduction mechanism, calculates electrode erosion heat fluxes and their peak powers caused under different discharge conditions. Calculation results indicate that arc joule heat is the main reason of electrode erosion when discharge current is not too high.*

*Streszczenie. Zbadano erozję elektrody w wyłącznikach gazowych przy wyładowaniach impulsowych. Przeprowadzono obliczenia przewodnictwa cieplnego oraz rozkład temperatury wokół elektrody. Stwierdzono że główną przyczyną erozji jest ciepło wyładowania łukowego. (**Badania mechanizmu przewodzenia ciepła na powierzchni elektrody wyłącznika gazowego**)*

Keywords: Field-distortion Gas Switch; Electrode Erosion; Erosion Mechanism; Erosion Thermal Mechanism
Słowa kluczowe: wyłącznik gazowy, erozja elektrod, przewodnictwo cieplne.

Pulse power technology has found wide application in high-power laser, Z-pinch, high-power microwave and material surface modification and applications of this technology in these fields, in turn, has lent impetus to its development towards higher reliability, higher power and higher repetitive frequency. [1-3] Gas switch is a crucial element of pulse power devices, and its technological advance also boosts the further development of pulse power technology. Pulse power technology requires the switch to operate in high power, transient state heavy current environment, and it is easy to form etch pit on electrode surface. Electrode etch pit is the important factor results in reduction of switch self breakdown voltage and increase in triggering jitter, directly impacting the service performance and reliability of switch and reducing service life of switch. Therefore, electrode erosion is a key restrictive factor in high-power gas switch development and application [4-9].

Discharging in gas switch causes the temperature of electrode materials at arc-electrode contact point to suddenly rise, the electrode materials near contact point to rapidly melt or vaporize when the temperature reaches its melting or vaporizing point, and lead to removal of electrode materials and form etch pit, this process is called electrode erosion [7,10-13]. Domestic and foreign researches indicate that the energy balance at the electrode surface [14,15]. Electrode material removal, that is, electrode erosion, is caused by external heat sources when gas switch discharges. Therefore, study on external heat fluxes and thermal conduction mechanism on the electrode surface is necessary to etch pit calculation and switch lifetime research.

According to one dimensional equation of heat conduction and thermal equilibrium equation near the electrode surface, heat fluxes and their peak powers caused under different discharge conditions are calculated in this paper.

1. Electrode Surface Thermal Conduction Mechanism

1.1 heat conduction equation

Electrode erosion is caused by external heat conduction, and the temperature distribution inside electrode at the arc-electrode contact point can be calculated by one-dimensional heat conduction equation [12,16-19].

$$\frac{\partial T_m}{\partial t} - \frac{\partial^2 T_m}{\partial z^2} = 0 \tag{1}$$

Initial conditions:

$$T_m(z,0) = 293K \tag{2}$$

Boundary conditions:

$$\frac{\partial T_m(0,t\ )}{\partial z} = \frac{q_{cond}}{k} \tag{3}$$

(4)

$$(-k_s \frac{\partial T_m(z,t)}{\partial z}\Big|_{z_l} + k_l \frac{\partial T_m(z,t)}{\partial z}\Big|_{z_l+dz_l}) \cdot dt = L_m \rho dz_l$$

$$(q_{cond} + k_l \frac{\partial T_m(z,t)}{\partial z}\Big|_{z_v+dz_v}) \cdot dt = L_b \rho dz_v \tag{5}$$

where: T_m – electrode temperature at different moments and different depth, $m = k/\rho c$, q_{cond} – heat flux sum conducting into electrode, L_m – latent heat of fusion, L_b – latent heat of vaporization, z_v – vaporization front of previous moment, z_l – fusion front of previous moment, dz_v – vaporization length of current moment, dz_l – melting length of current moment. The fusion front and vaporization front are shown in Figure 1.

The above equations are parabola partial differential equation, equation of heat conduction is homogeneous, but boundary conditions are nonhomogeneous. Therefore, it is quite difficult to solve directly, and finite difference method is used for solving [20,21].

1.2 Electrode heat conduction Mechanism

Domestic and foreign researches indicate that the energy balance at the electrode surface [14,15]. Value of conduction heat flux q_{cond} is equal to the difference between the heat fluxes flowing in and flowing out of the electrode surface. The heat fluxes and their relations can be represented with the equation below.[12]

$$q_{cond} = q_{ij} + q_{ch} + q_j + q_{arc} + q_c + q_r - q_{ev} \tag{6}$$

where: q_{ij} – electrode joule heat, q_{ch} – chemical reaction heat, q_j – plasma jet, q_{arc} – arc joule heat, q_c – the heat conduction by charged particle bombardment, q_r – radiant heat, q_{ev} – the net loss due to evaporation.

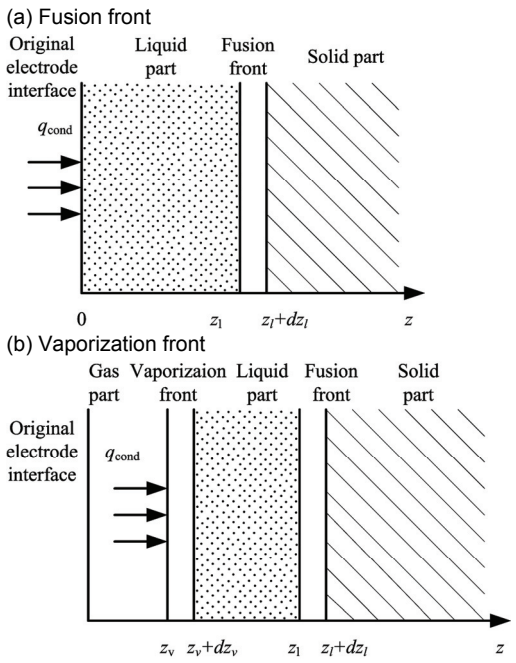

Fig. 1 Electrode Material Phase Transition Diagram

Electrode joule heat q_{ij} is generated by electrode resistance and electrode surface resistance, the temperature rise $\triangle T$ is as shown in Cramer & Roman formula: [22]

$$\Delta T = \frac{\eta J^2 t_s}{\rho c} \tag{7}$$

where: η – the electrical resistivity, J – current density, t_s – discharge time. The temperature rise caused by electrode joule heat is still very little. When peak current is not too high, temperature rise $\triangle T$ < 1K, therefore it is usually ignored.

The influences of chemical reaction heat q_{ch} on electrode erosion are in many aspects. Part of materials on electrode surface participated in chemical reaction, which will promote electrode erosion; if chemical reaction is mainly based on exothermic reaction, temperature of electrode surface will rise, and it will promote the proceeding of chemical reaction, forming a virtuous circle in favor of chemical reaction and accelerating electrode erosion; if chemical reaction based on endothermic reaction, then electrode erosion will be retarded. Only when peak current is very big and temperature of electrode surface is much high, the chemical reaction can be intense and have big impact on electrode erosion [23-25]. In this paper, the requirement for peak current is not too high. Therefore, the impact of chemical reaction on electrode erosion is ignored.

During discharge, there are good deal of anion, cation and electron in arc plasma, which is constantly accelerating under the electric field and bombarding electrode surface, delivering own kinetic energy and potential energy to electrode surface, and transforming into thermal energy [26]; or removing from electrode in the form of electron and taking energy away [9,27].

When gas switch discharges, arc conducts large quantity of heat to electrode surface. Arc joule heat q_{arc} is an important heat conduction mechanism.

Generally, little charged particle generates during discharge. Therefore, the heat flux q_c due to charged particle bombarding to electrode surface is low. In addition, radiant heat q_r is also very low. They are usually ignored [12].

The heat flux q_{ev} [14] is the energy required for vaporization of electrode material, and will be counted in boundary conditions, which is Formula (5).

2) **Calculation of heat fluxes**

In heat fluxes conducted to electrode surface, except arc joule heat q_{arc}, calculation equation of others conducted to cathode and anode is not same.

Calculation formula of arc joule heat q_{arc} is [15]:

$$q_{arc} = k_p V_{arc} J \tag{8}$$

where: k_p – the proportion of energy conducted to electrode surface by arc and absorbed by electrode surface, V_{are} – arc voltage drop, J – current density.

(1) Calculation of anode heat fluxes

On anode surface, plenty of electrons transform kinetic energy and potential energy into thermal energy through bombarding anode surface, and make temperature of anode surface to rise, which is one of major heat fluxes conducted into anode surface. Meanwhile, small quantity of anion bombards anode surface, but it is very small, and energy conducted into anode is little as well and can be ignored.

Equation of heat balance of anode surface is [14,28,29]

$$q_{cond} = q_{arc} + q_e \tag{9}$$

where: q_e – the incidence electron heat flux.

$$q_e = |J|[\frac{5}{2}\frac{k_B}{e}(T_g - T_a) + \phi_a + V_a] \tag{10}$$

where: k_B – Boltzmann constant, e – magnitude of electronic charge, T_g – temperature of gas between electrode and arc, T_a – electrode surface temperature, ϕ_a – work function of anode material and ϕ_a = 4.5V for copper, V_a – anode voltage drop in the non-LTE (local thermal equilibrium) layer in front of the anode, when discharge peak current is not too high, V_c + V_a = 17.5V, V_a = 2.5V [14,30].

Generally, the term $5k_B(T_g\text{-}T_a)/2e$ is relatively small and can be ignored. q_e can be simplified as:

$$q_e = |J|(\phi_a + V_a) \tag{11}$$

(2) Calculation of cathode heat fluxes

Particle near cathode is mainly cation, which bombards cathode surface and transforms kinetic energy and potential energy into thermal energy under the effect of electric field, and is one of major heat conducted into electrode surface. In addition, there are also small quantity of anion will breaks through potential barrier, and bombard cathode surface, but the quantity is very small and can not be considered.

During discharging, there are plenty of electrons overflowing from cathode surface. Electrons escape from cathode and transform thermal energy into kinetic energy, which is one of the major heat fluxes conducted out of electrode surface.

Heat conducted to cathode surface is [14,31]:

$$q_{cond} = q_{arc} + q_{ion} - q_{ejet} \tag{12}$$

where: q_{ion} – energy brought due to ion bombarding cathode surface, q_{ejet} – energy taken away due to ejection of cathode electron.

$$q_{ion} = J_i(V_c + V_i - \phi_c + \frac{5k_B}{2e}T_c) \tag{13}$$

where: V_c – voltage drop on cathode sheath and V_c=15V for copper [14,30], V_i – ionization energy of plasma gas and V_i=7.73V for copper [14,30], ϕ_c – work function of cathode material and ϕ_c=4.5V for copper, T_c – the cathode spot

temperature, J_i – ion current density, some researches indicate that total current density $J=|J_i|+|J_e|$, J_e – electron current density, meeting $|J_e|/|J|=0.78$ [14,32].

Generally, the term $5k_BT_c/2e$ is very small, can be ignored. q_{ion} can be simplified as:

$$q_{ion} = J_i(V_c + V_i - \phi_c) \tag{14}$$

$$q_{ejet} = |J_e|\phi_c \tag{15}$$

2. Results and Analysis of Experiments and Calculation

2.1 Experiment platform

This paper adopts a field-distortion gas switch widely used in pulsed-power technology, and the structure of the switch is shown in Figure 2.

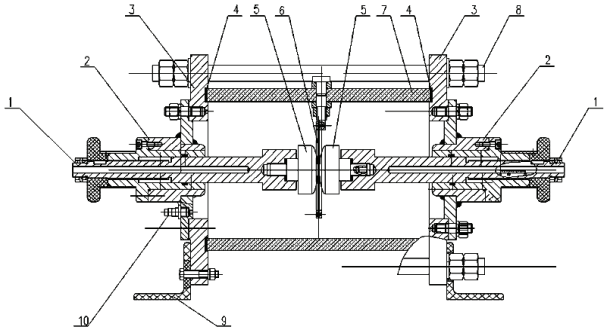

Fig. 2 Field-distortion Gas Switch

1-tunable electrode bar with dial; 2-slipcover; 3-end cover; 4-sealing ring; 5-main electrode; 6-trigger electrode; 7-transparent shell; 8-fixed screw unit; 9- bedplate; 10-charge and discharge gas terminal

The main electrodes and trigger electrode are coaxially placed inside the gas switch while trigger electrode is located in the center of main electrodes. Electrode surface is spherical crown shaped with radius of 78mm. The gap between main electrodes is 11mm and the trigger electrode thickness is 1mm. All the electrodes are made of brass. Electric-field non-uniformity coefficient is 1.115. In the experiment the switch is filled with SF_6 gas in the range from 0.1MPa to 0.4MPa, the charge voltage $\pm U_0$ and trigger voltage U_1 are applied onto the main electrodes and trigger electrode of the switch, respectively.

In order to research thermal conduction mechanism and electrode erosion property when discharge current is not too high, single nanosecond pulse current generation device has been established as shown in Figure 3.

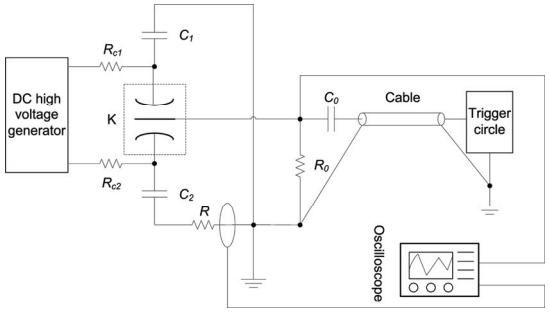

Fig. 3 Structure of Gas Switch Experiment Platform

Experiment platform consists of gas switch, positive and negative high voltage DC generator, capacitor, trigger system, vacuum pump, gas supply system (high pressure gas cylinder adopted in this paper), voltage and current measurement equipment, oscilloscope and so on. Bipolar DC high voltage source charges less than 100kV DC voltage in two capacitors through 2MΩ protective resistance. The values of two capacitors are same. Trigger system will provide trigger pulse voltage on trigger electrode for switch breakdown when DC changing process is completed. Discharge current is measured by Rogowski coil, and the measured result is displayed on oscilloscope and saved for further processing. Before experiment, vacuum pump extracts the gas in switch, and then SF_6 gas is charged in switch through gas cylinder. In order to remove other gas as much as possible, increase concentration of SF_6 gas in switch as much as possible to ensure reliable experiment results, the gas discharging process mentioned above is usually performed 4-5 times.

The discharge current waveforms under 5 discharge conditions are as shown in Figure 4.

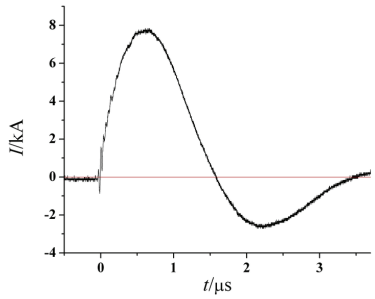

Fig. 4 Diagram of Discharge Current Waveforms

According to Figure 4, current waveforms half cycles are about 1.5μs, and its time is less than 3.5μs.

2.2 Heat fluxes calculation results and analysis

1) Calculation and analysis of external heat fluxes

According to the previous analysis, input and output heat fluxes on electrode surface mainly includes electrode joule heat q_{ij}, arc joule heat q_{arc}, plasma jet q_j and heat flux q_{ev} that is taken away from electrode surface when electrode material vaporizes and removes out, in which q_j includes ion collision electrode heat flux q_{ion}, the incidence electron heat flux q_e and energy taken away by electron escape from electrode surface q_{ejet}; q_{ev} is integrated into vaporization boundary conditions.

Electrode joule heat of q_{ij} is much less than total input heat flux. When discharge current waveform is as shown in Figure 4(a), heat flux q_{ij} only accounts for $1/10^5$ of total heat flux. In addition, when peak current I_m < 40kA, temperature rise $\triangle T$ < 1K. Therefore, impact of q_{ij} is generally ignored.

Three heat fluxes including arc heat conduction q_{arc}, et al, and total heat flux are as shown in Figures 5 and 6.

When peak current I_m<40kA, arc heat conduction q_{arc} accounts for over 90% of total heat flux, and heat power is also over 90% of total heat power, belonging to main heat flux required for electrode erosion; plasma ejection q_j is relatively low, only accounting for about 1%. Some foreign experiments researches indicate that [12], when peak current I_m>200kA, plasma jet accounts for about 60% of total heat flux; but when I_m<100kA, energy due to plasma jet is usually very small. Figure 5 and Figure 6 show that as peak current increases, heat flux q_{ev} increases and the proportion accounting for total heat flux gradually increases, from about 60% at 8.5kA to 50% at 40kA. Therefore, energy is mainly used for vaporization of electrode material, and exports from electrode surface as vaporized electrode material removal.

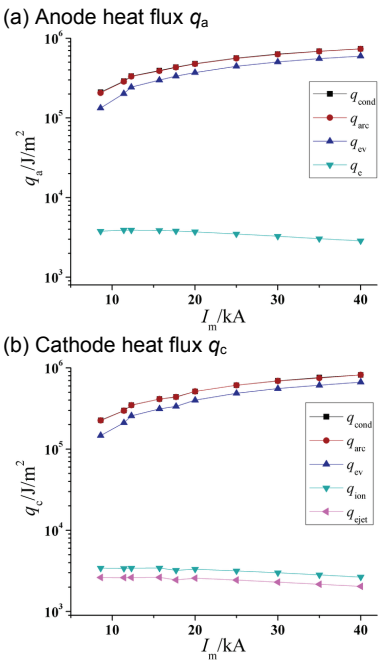

Fig. 5 Three Components of Heat Sum and Total Heat Sum during Erosion (total heat flux is not calculated in q_{ev})

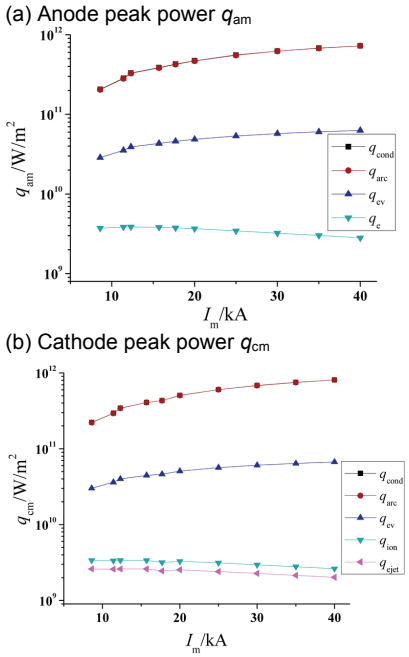

Fig. 6 Three Components of Heat Peak Power and Total Heat Peak Power during erosion

2) Solid particle removal

When electrode materials remove from electrode surface permanently, etch pit will be formed on electrode surface. Materials removal has four forms: charged particle, vapor, liquid and solid. Therefore, volume of electrode erosion is [12,27]:

$$V = k_{pr}V_p + k_{vr}V_v + k_{lr}V_l + k_{sr}V_s \quad (16)$$

where: V_p, V_v, V_l, V_s – in turn volume of charged particle, vapor, liquid and solid; k_{pr}, k_{vr}, k_{lr}, k_{sr} – in turn removal coefficients of charged particle, vapor, liquid and solid, and may vary from 0 to 1.

When peak current and electric quantity is relatively low, the temperature near electrode surface is relatively low and solid particle removes from electrode surface, as shown in Figure 7. Figure 7(a) shows that there is a small round pit with uneven bottom surface, which may be generated through liquid back flow on etch pit side wall in the stage of cooling and solidification after solid particle removes out; Figure (b) shows that a small pit with irregular shape and uneven bottom surface; Figure (c) shows that small pits with shape similar to round and uneven bottom surface. Such etch pits are not found when the current is large.

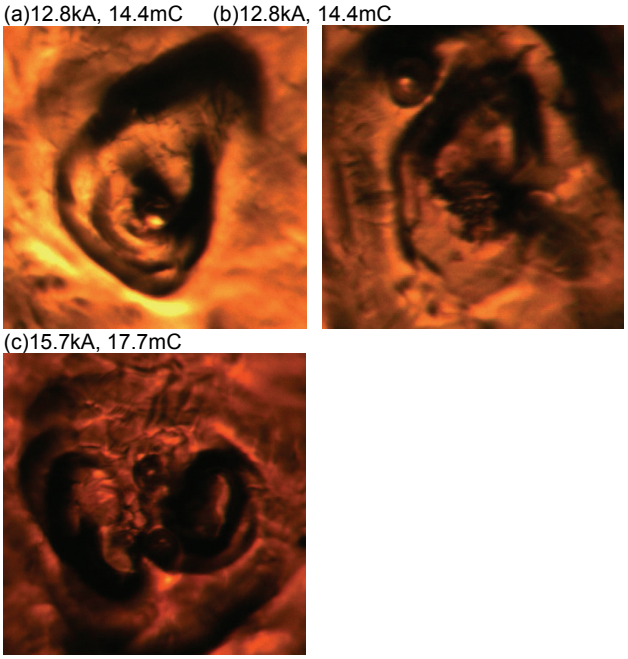

Fig. 7 Photo of Bottom of Electrode Etch Pit

When peak current is from 8kA to 16kA and electric quantity is from 12mC to 18mC, probability of solid removal is relatively big. Maximum probability of solid removal occurs when peak current is 12.8kA and electric quantity is 14.4mC, and small pits on the bottom surface of etch pit are observed in about 2/5 experiments. Shape and depth of solid removal has big randomness. They are close to roundness (such as Figure 7(c)) or irregular shape (such as Figure 7(b)). Pit depth of solid removal is more than 6μm as shown in Figure 7(a), and that only is 1.6μm as shown Figure 7(b). When solid removal exists, etch pit depth deviation is big too. For example, when peak current is 12.8kA and electric quantity is 14.4kA, average value of etch pits depth is 7.92μm and maximum deviation is 4.92μm, reaching 62.1% of average value. However, when peak current is 20kA and electric quantity is 28.5mC (solid removal has not been observed), average value of etch pits depth at this time is 12.6μm and maximum deviation is 2.19μm, accounting for only 17%. Therefore, the occurrence probability of solid removal is big, and its shape and depth are irregular, which is related to occasional defects of electrode surface material, the temperature near electrode surface, oscillation wave, thermal stress and so on.

3. Conclusion

Based on heat conduction Mechanism, heat fluxes and their peak powers have been calculated under different discharge conditions.

When peak current is not too high, thermal energy has been calculated based on thermal conduction mechanism. Calculation results indicate that heat fluxes supplied for erosion are mainly derived from arc joule heat, accounting for over 90%. The impact of plasma jet and other heat

fluxes on erosion is small, accounting for only around 1%. Energy is mainly used for vaporization of electrode materials, and energy consumes by vaporization accounts for 60%-80% of total heat flux within the range of discharge parameters researched in this paper.

The research also finds that when peak current is from 8kA to 16kA and electric quantity is from 12mC to 18mC, electrode materials are possible to remove from electrode surface in the form of solid particle, at this time, deviation of etch pit depth and shape is big.

REFERENCES

[1] Qiu AC. The Development of Technology for Pulsed X ray Simulators[J]. Engineering Science, 2000, 2 (09): 24-28.

[2] Mesyats GA. Pulsed Power[M]. New York: Kluwer Academic, 2004.

[3] Neau EL. Environmental and Industrial Applications of Pulsed-Power Systems[J]. IEEE Transactions on Plasma Science, 1994, 22 (1): 2-10.

[4] Musschoot J, Depla D, Buyle G, et al. Influence of the geometrical configuration on the plasma ionization distribution and erosion profile of a rotating cylindrical magnetron: a Monte Carlo simulation[J]. Journal of Physics D-Applied Physics, 2006, 39 (18): 3989-3993.

[5] Chau SW, Hsu KL, Lin DL, et al. Experimental study on copper cathode erosion rate and rotational velocity of magnetically driven arcs in a well-type cathode non-transferred plasma torch operating in air[J]. Journal of Physics D-Applied Physics, 2007, 40 (7): 1944-1952.

[6] Peters J, Yin F, Borges CFM, et al. Erosion mechanisms of hafnium cathodes at high current[J]. Journal of Physics D-Applied Physics, 2005, 38 (11): 1781-1794.

[7] Donaldson AL, Hagler MO, Kristiansen M, et al. Electrode Erosion Phenomena in a High-Energy Pulsed Discharge[J]. IEEE Transactions on Plasma Science, 1984, 12 (1): 28-38.

[8] Donaldson AL, Kristiansen M, Watson A, et al. Electrode Erosion in High-Current, High-Energy Transient Arcs[J]. IEEE Transactions on Magnetics, 1986, 22 (6): 1441-1447.

[9] Liau VK, Lee BY, D Song K, et al. The influence of contacts erosion on the SF_6 arc[J]. Journal of Physics D-Applied Physics, 2006, 39 (10): 2114-2123.

[10] Watson A, Donaldson AL, Ikuta K, et al. Mechanism of Electrode Surface Damage and Material Removal in High-Current Discharges[J]. IEEE Transactions on Magnetics, 1986, 22 (6): 1799-1803.

[11] Mcclure GW. Plasma Expansion as a Cause of Metal Displacement in Vacuum-Arc Cathode Spots[J]. Journal of Applied Physics, 1974, 45 (5): 2078-2084.

[12] Donaldson AL. Electrode erosion in high-current, high-energy transient arcs[D]. Lubbock: Texas Tech University, 1991.

[13] Butkevich GV, G. S. Belkin, Vedeshenkov NA. Electrical erosion on heat flux and duration of current flow[J]. Sov phys Tech Phys, 1971, 15 (7): 1167-1170.

[14] Zhang JL, Yan JD, Fang MTC. Electrode evaporation and its effects on thermal arc behavior[J]. IEEE Transactions on Plasma Science, 2004, 32 (3): 1352-1361.

[15] Donaldson AL, Kristiansen M. Utilization of a thermal model to predict electrode erosion parameters of engineering importance[C]. San Diego: IEEE Conference Record of the 1990 Nineteenth Power Modulator Symposium, 1990: 265-269.

[16] Belkin GS. Procedure for Calculating Rosion of Heavy-Current Contacts by Arcing[J]. Electrical Technology, 1972, 5: 151-155.

[17] Yu CM. Heat conduction and its numerical analysis[M]. Beijing: Tsinghua University Press, 1981.

[18] Guo DR. Heat conduction equation and its solution[M]. Beijing: China Higher Education Press, 1991.

[19] Lou M, Jiang CS, Chang AB. Study on mechanism of electrode erosion of high-power gas spark gap switch[J]. High Power Laser & Particle Beams, 2004, 16 (6): 781-786.

[20] Croft DR. Finite difference methed for heat transfer calculation[M]. Beijing: Metallurgical Industry Press, 1982.

[21] Gao BQ. Finite difference time-domain method[M]. Beijing: National Defence Industrial Press, 1995.

[22] Cramer KR, Roman WC. Electrode Design Based on Transient Thermal Analysis[J]. Mechanical Engineering, 1970, 92 (5): 75-79.

[23] Gordon LB, Kristiansen M, Hagler MO, et al. Material Studies in a High-Energy Spark Gap[J]. IEEE Transactions on Plasma Science, 1982, 10 (4): 286-293.

[24] Behrisch R. Surface Erosion from Plasma Materials Interaction[J]. Journal of Nuclear Materials, 1979, 85-6 (Dec): 1047-1061.

[25] Szente RN, Munz RJ, Drouet MG. Effect of the Arc Velocity on the Cathode Erosion Rate in Argon Nitrogen Mixtures[J]. Journal of Physics D-Applied Physics, 1987, 20 (6): 754-756.

[26] Pamela J, Ongena J, Contributors JE. Overview of JET results[J]. Nuclear Fusion, 2005, 45 (10): S63-S85.

[27] Donaldson AL, Kristiansen M. Electrode Erosion as a Function of Electrode Materials in High Current, High Energy Transient Arcs. Pulsed Power Conference: Monterey, California, 1989: 83-86.

[28] Gleizes A, Bouaziz M, Gonzalez JJ, et al. Influence of the anode material on an argon arc[J]. Ieee Transactions on Plasma Science, 1997, 25 (5): 891-896.

[29] Zingerman AS, Kaplan DA. Electric Erosion of an Anode as a Function of Interelectrode Distance[J]. Soviet Physics-Technical Physics, 1958, 3 (2): 361-367.

[30] Coulombe S, Meunier JL. A comparison of electron-emission equations used in arc-cathode interaction calculations[J]. Journal of Physics D-Applied Physics, 1997, 30 (20): 2905-2910.

[31] Zhou X, Heberlein J, Pfender E. Theoretical-Study of Factors Influencing Arc Erosion of Cathode[J]. Ieee Transactions on Components Packaging and Manufacturing Technology Part A, 1994, 17 (1): 107-112.

[32] Yokomizu Y, Matsumura T, Henmi R, et al. Total voltage drops in electrode fall regions of SF6, argon and air arcs in current range from 10 to 20000 A[J]. Journal of Physics D-Applied Physics, 1996, 29 (5): 1260-1267.

***Authors**: dr Hu Wang, School of Electrical Engineering, Xi'an Jiaotong University, China, E-mail: tiger.king@stu.xjtu.edu.cn; prof. dr Qiaogen Zhang, School of Electrical Engineering, Xi'an Jiaotong University, China, E-mail: hvzhang@mail.xjtu.edu.cn; dr Xuandong Liu, Xi'an Jiaotong University, China, E-mail: liu.xuandong@stu.xjtu.edu.cn; prof. Academician of chian engineering academy, Aici Qiu, School of Electrical Engineering, Xi'an Jiaotong University, China.*